

Rashba spin splitting and Dirac fermions in monolayer PtSe₂ nanoribbons

Bo-Wen Yu and Bang-Gui Liu*

*Beijing National Laboratory for Condensed Matter Physics,
Institute of Physics, Chinese Academy of Sciences, Beijing 100190, China and
School of Physical Sciences, University of Chinese Academy of Sciences, Beijing 100049, China*
(Dated: November 17, 2023)

Two-dimensional (2D) semiconducting transition metal dichalcogenides have potential applications in various fields. Recently, it is shown experimentally and theoretically that monolayer PtSe₂ nanoflakes with neutral edges are stable. Here, we study PtSe₂ nanoribbons with the stable zigzag edges through first-principles investigation and find Rashba spin splitting and gapped relativistic electron dispersion in their valence and conduction bands near the Fermi level. Our analysis of atom-projected band structures and densities of states indicates that the part of bands originates mainly from the edges of the nanoribbons. It is also shown that there exists a SU(2) spin symmetry in both valence and conduction band edges, which implies persistent spin helix along the edges. Furthermore, we can achieve a Dirac electron model for an edge by combining the valence and conduction bands when the inter-edge interaction is weak. These electronic systems could be useful for designing high-performance spintronic and optoelectronic applications.

I. INTRODUCTION

Achievement of graphene arouses the interest of two-dimensional materials for both practical applications and theoretical research[1–3]. Transition metal dichalcogenides (TMDs) as typical a kind of 2D materials has various amazing properties in the field of high-performance electronic, spintronic, and optoelectronic devices[4–6]. Recently, monolayer platinum diselenide (PtSe₂) which is found with a stable monolayer structure and grown successfully on various surface attracted interest for a variety of potential applications [7–11]. Further exploration of PtSe₂ indicate that there are many intriguing properties such as piezoresistivity, spin-layer locking and other properties[12–15]. Moreover it is acknowledged that PtSe₂ has potential applications in electronic and optoelectronic devices[11, 16–21]. However, another typical TMD material, WSe₂ and WTe₂ which has the similar structures to PtSe₂ shows topological properties and edge state [22, 23]. So the broken covalent bonds at the edges of PtSe₂ can also cause the new electronic states [10].

In this work, the model of PtSe₂ nanoribbon with zigzag edge is built to investigate the electronic properties of the edge state. Calculations indicate that edge state exists and the dispersion relation of the band near Fermi level fit the formula of relativity. Further analysis of the projected band and density of states show the origin of the edge state and the spin split which is related to the Rashba effect. The coupling between the atom and spin might lead to the persistent spin helix which is the basic property to be used in the spintronic devices.

II. METHODOLOGY

The first-principles calculations are performed with the projector-augmented wave (PAW) method within the density functional theory[24], implemented in the Vienna Ab-initio simulation package software (VASP) [25]. The generalized gradient approximation (GGA) by Perdew, Burke, and Ernzerhof (PBEs)[26] is used as the exchange-correlation functional. The self-consistent calculations are carried out with a Γ -centered ($12 \times 1 \times 1$) Monkhorst-Pack grid[27]. The kinetic energy cutoff of the plane wave is set to 450 eV. The convergence criteria of the total energy and force are set to 10^{-6} eV and 0.01 eV/Å. The spin-orbit coupling (SOC) is applied in the calculation of band structure and lattice structure.

III. RESULT AND DISCUSSION

A. Monolayer structures and Edges

2D PtSe₂ belongs to the material family of TMDs. Usually monolayer TMDs have two kinds of stable monolayer structures, H-phase and T-phase. Previous theoretical and experimental work indicates that the T-phase is the most stable one for the layered PtSe₂. The T structure of PtSe₂ without any strain or defects has C₃-centered symmetry and there are six Se atoms near each Pt atom in the lattice of PtSe₂. Similar to graphene which also has the 120° rotational symmetry structure, there are two types of the edge, armchair edge and zigzag edge. But the situation of the edge of PtSe₂ is more complex than graphene because the monolayer PtSe₂ has two different atoms. The armchair edge is along the line of Pt-Se-Se-Pt, which can separate the monolayer under the premise of keeping the stoichiometric ratio of PtSe₂ unchanged. The zigzag edge is different from the armchair edge and there are 3 kinds of edge along the zigzag direction. If the dividing line along the zigzag direction

* bgliu@iphy.ac.cn

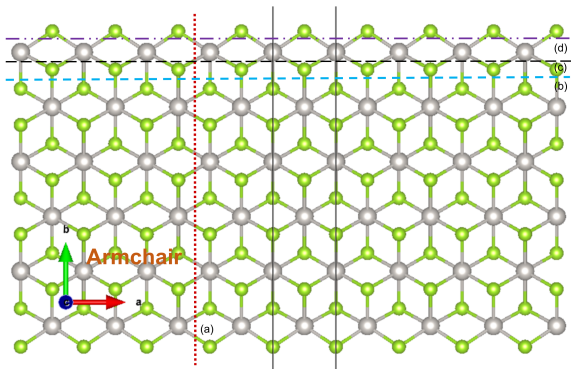


FIG. 1: The structure of the PtSe₂ nanoribbon. (a) The dividing line for armchair edge. (b) The dividing line for model of 9 unit cells wide nanoribbon with zigzag edge. (c) The dividing line for the zigzag edge of Se. (d) The dividing line for the zigzag edge of Pt.

crosses the Pt-Se bond, there will be two zigzag edges, one is the edge of Pt and the other is the edge of Se. These kinds of edges maintain the stoichiometric ratio of PtSe₂ and there will be net charge on the edge and it is very easy for the bonds near the edge to reconstruct. And if the dividing line along the zigzag direction partially bypass the Pt-Se bond and pass between two Se-Se lines and there will be a zigzag edge with the correct stoichiometric ratio of PtSe₂. This kind of edge can avoid the net charge and bond reconstruction on the edge. A model of PtSe₂ nanoribbon which has 30 atoms and a 20 Å vacuum layer is proposed in order to compare the energy of the zigzag with correct edge stoichiometric ratio and armchair edge. The result indicates that the zigzag edge which has the correct edge stoichiometric ratio is more stable than the armchair edge.

In order to study the properties of the edge of PtSe₂, a nanoribbon model 10 PtSe₂ cells wide is created. The edge of this model is the zigzag edge which keeps the correct edge stoichiometric ratio to ensure the balance of charge on the edge. The outermost atoms of the nanoribbon in this model are Se atoms on the both sides of the zigzag edge. They have two nearest neighbor Pt atoms and the each outermost Pt atom has 5 nearest neighbor Se atoms, 2 outside and 3 inside. There are 10 Pt atoms and 20 Se atoms in the model and the 2 Pt atoms and 2 Se atoms which are located in the nanoribbon center are fixed during structure optimization calculations. The result indicates no drastic changes in the position of atoms and bond structure compared to the structure of the monolayer PtSe₂ without edge. The changes are mainly concentrated in the length of the outermost Se-Pt bond which is 2.7% shorter than the Pt-Se bonds in the monolayer or the bonds near the middle of nanoribbon.

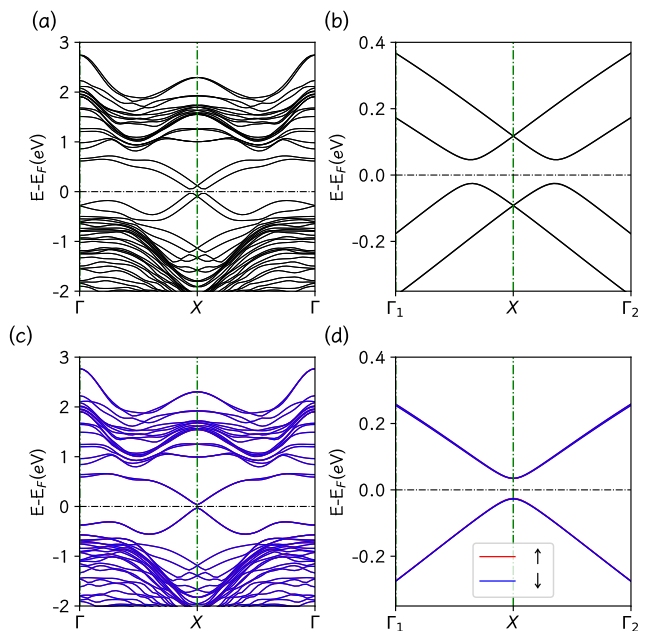


FIG. 2: The band structure with and without SOC of PtSe₂ nanoribbon which contain 10 Pt atoms and 20 Se atoms. (a) the entire Brillouin zone without SOC (b) partial enlargement of (a). (c) the band structure without SOC. (d) partial enlargement of (c).

B. Electronic structures and band dispersion

The main electronic structures of PtSe₂ nanoribbon which contains 10 cells of PtSe₂ is shown in Fig. 2. It is clear that this nanoribbon is a direct-gap semiconductor and the CBM and VBM are located at the points near the X in k space. The semiconductor gap is 0.0721 eV and the band is axially symmetrical without considering other factors such as spin and orbital projection. So there are two groups of CBM and VBM which are located on both sides of the X point. And the CB and VB changes linearly with k in a relatively large range which occupy one third of the total Brillouin zone.

However, the most noteworthy fact from the partial enlargement of band structure is that the dispersion relation of the band edge is similar to the massive relativistic dispersion relation $E = \pm\sqrt{p^2 + m^2}$. The result of the quantitative fitting indicates that the dispersion relation conforms to the relativistic energy-momentum formula $E^2 = a(k - k_0)^2 + b$ in high quality. The k_0 is the location of VBM or CBM in Brillouin zone. For VBM k_0 is $4.4825 \times 10^{-2} \text{ \AA}^{-1}$ and for CBM k_0 is $4.4198 \times 10^{-2} \text{ \AA}^{-1}$ (the coordinate origin is at X). There is also little anisotropy near the band edge and the fitting parameters of the two direction, toward the X and Γ , differ slightly. The parameters a for VBM are $4.5594 \text{ eV}^2 \cdot \text{\AA}^2$ for Γ direction and $4.8375 \text{ eV}^2 \cdot \text{\AA}^2$ for X direction. The parameters a for CBM are $3.3565 \text{ eV}^2 \cdot \text{\AA}^2$ for Γ direction and $4.4009 \text{ eV}^2 \cdot \text{\AA}^2$ for X direction. The parameters b

for CBM are 4.5594×10^{-3} eV for Γ direction and 3.1647×10^{-3} eV for X direction. The parameters b for VBM are 2.9174×10^{-3} eV for Γ direction and 1.0780×10^{-3} eV for X direction.

C. Edge States

More exploration has been conducted to ensure the existence of edge state. Further analysis shows the fact that there are 8 degenerate bands near the Fermi level, 4 VBs and 4 CBs. These 8 bands are independent of the pack of other bands which indicates that they have different origins than others.

Fristly, the projected density of states is calculated to find out the origins of bands near Fermi level. The 30 atoms who make up the PtSe₂ nanoribbon are divided into 10 groups from left to right according to their position in the lattice. Each Pt atom and their nearest 2 Se atoms is in the same group. The density of states is projected to these 10 groups and the result shows that the DOS near is mainly contributed by group 1 and group 10 which are located at the edge of the nanoribbon with a small contribution from group 2 and group 9 which are near the edge of the nanoribbon. The groups far from the edge basically have no contribution to the DOS near the Fermi level.

Furthermore, the projected band structure is calculated to ensure these 8 bands are from the atoms of edges. It is found that the two degenerate orbits are one from the leftmost Pt atom and the other one from the rightmost Pt atom for both VB and CB bands. The relationship between edge, atoms and spin will be discussed in the following section.

It is acknowledged that the width of the nanoribbon can also have influence on the properties of the band structure. So the models of PtSe₂ nanoribbon ranging from 3 to 10 PtSe₂ cells are studied to investigate the influence of the width of the nanoribbon on the band structure. The band structure shows that the basic features of the edge state still remain, even with very narrow width. The band gap increases as number of PtSe₂ unit cells increase. And the average distance between the two VBM and CBM in k space remains the same when the number of PtSe₂ unit greater than 4. What is more instresting is that the band structure changes change differently for the odd and even number of PtSe₂ cells. For odd number of PtSe₂ cells, the band change is more obvious than for even number of PtSe₂ cells when the N decreases. The most significant change is that there is a split at X point for both VB and CB. For N = 9, the energy split is 0.0011 eV (VB) and 0.0037 eV (CB) which is small enough to ignore. But for N = 3, the energy split is 0.1476 eV (VB) and 0.2727 eV (CB) which is large enough to subvert the band structure. However for N is even number, the energy split is still small even N = 4 which has 0.0006 eV (VB) and 0.0007 eV (CB) energy split. And for N = 10, there is no energy split at X point for neither VB or CB.

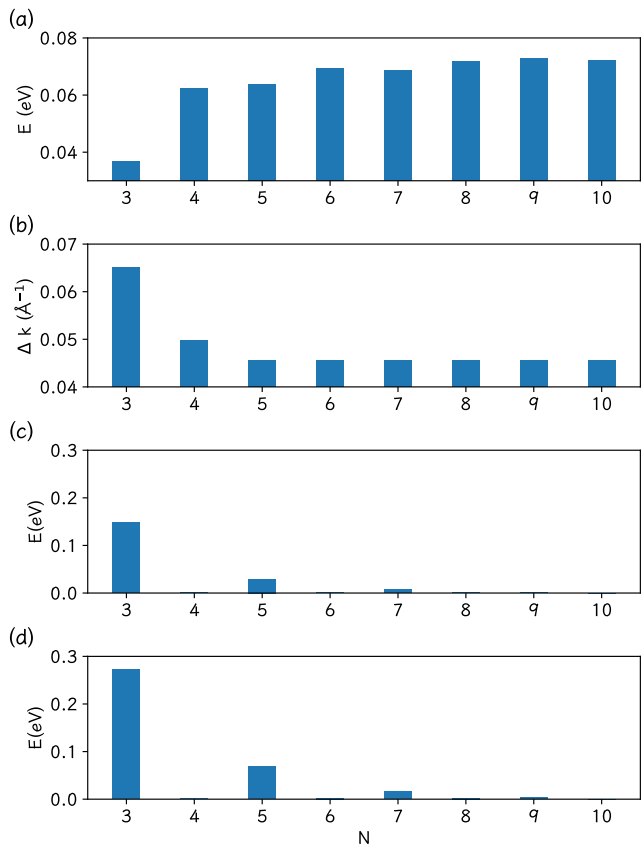


FIG. 3: (a) The gap of PtSe₂ nanoribbons with different widths. N is the number of PtSe₂ cells. (b) The average distance between the two CBM and VBM in k space. (c) The energy difference of VB at X point. (d) The energy difference of CB at X point.

It is believed that the difference between the odd and even number is due to the symmetry difference of the two kind of structure of the nanoribbon. For N is odd number, there is inversion symmetry in the lattice but there is no inversion symmetry in lattice of even number of PtSe₂ nanoribbon. The lack of symmetry might hinder the interaction of electrons between both sides of the nanoribbon, which can keep the band structure no change even when N is small.

D. Rashba spin splitting and SU(2) symmetry

Here the spin properties of the edge states from PtSe₂ nanoribbon are studied to understand the origin of behavior of the band structure and find out the potential applications of the PtSe₂ nanoribbon. Fristly, the band structure without SOC is calculated and the result indicates the fact that the CBM and VBM move to the X point and the 4 VB and 4 CB become degenerate. However, one of the main features, massive relativistic dispersion relation still keeps no change, which indicates that

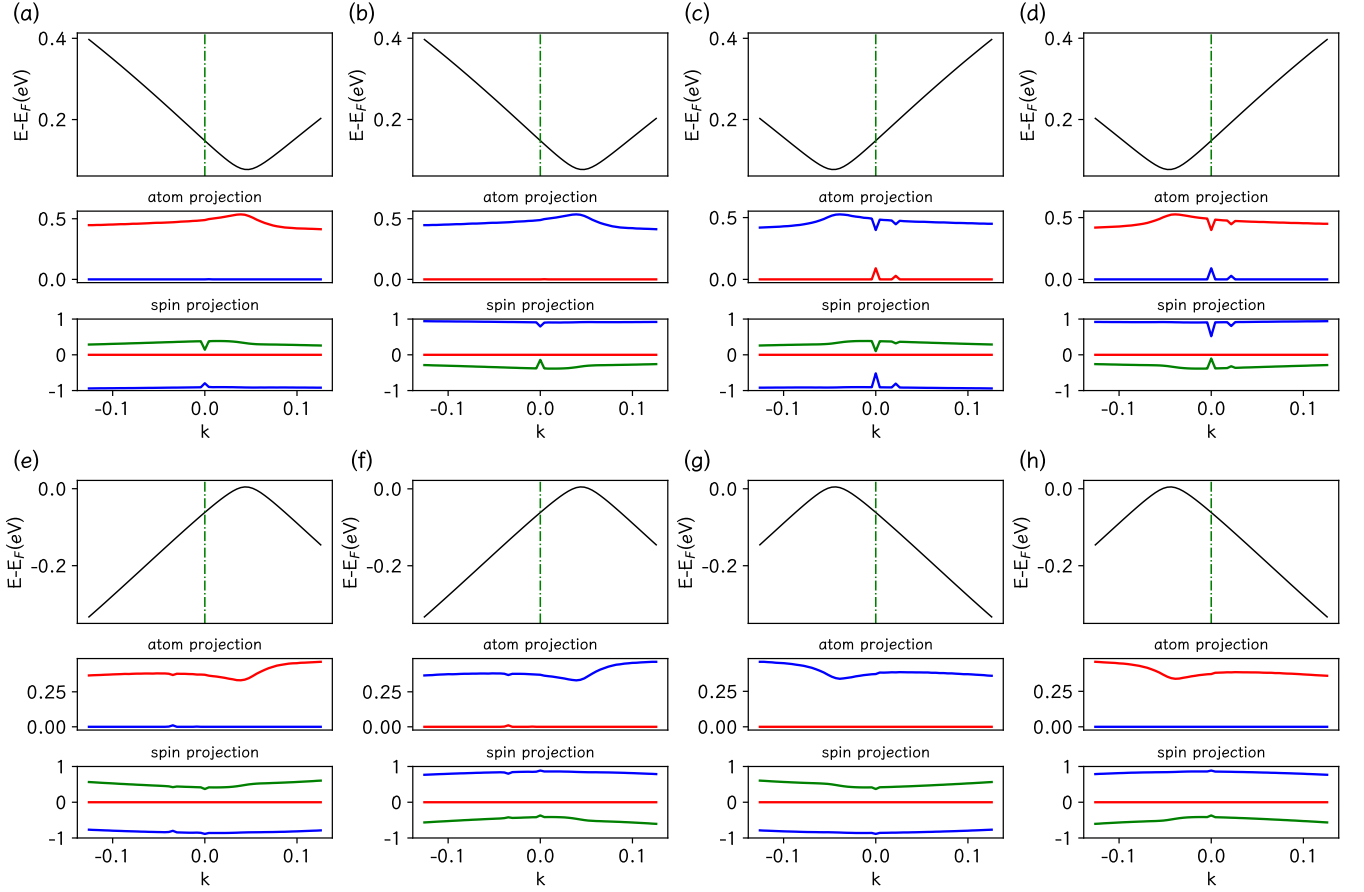


FIG. 4: The projection of atom or spin for 8 bands near X point. The red line in atom projection is the projection of Pt atom which is located at left edge of the nanoribbon. The blue line is the projection of Pt atom which is located at right edge of the nanoribbon. For spin projection, the red, green and blue means the S_x , S_y and S_z respectively. The origin of the coordinate axis is at X in k space.

the SOC is not the origin of relativistic dispersion. Further calculations are conducted to get more details about these 8 bands. The atom projection and spin projection is calculated and the 8 bands is regrouped according to the atom projection and spin projection. The result is shown in Fig. 4. For CB, the atom projection shows that the band (a) and band (d) are from the left edge of the nanoribbon. Their minimum values are respectively located to the left and right of point X in k space. Their spin projection indicates that they have spin in opposite direction. The spin, location of the band minimum and the position in real space coupled together. This feature appears not only in (a) (d), but also in (b) (e) for the right side of the nanoribbon, not only in CB but also in VB. The width of the nanoribbon is long enough to block the interaction between the two sides of the nanoribbon. So the electrons on both sides of the nanoribbon can be seen as independent. For the one side of the nanoribbon, there is a spin-split caused by SOC at X point according to the comparison between band structure with SOC and band structure without mentioned earlier. This spin-split make the band edge move toward different direction in

k space for the band with opposite spin, which is a typical feature of 1D Rushbar effect. So, according to the massive relativistic dispersion relation and the behavior of Rushbar effect, the Hamiltonian of this model reads

$$\hat{H} = \sum_k [\sqrt{\alpha_c^2(k + \gamma_c)^2 + m_c^2} c_{kc\uparrow}^\dagger c_{kc\uparrow} + \sqrt{\alpha_c^2(k - \gamma_c)^2 + m_c^2} c_{kc\downarrow}^\dagger c_{kc\downarrow} - \sqrt{\alpha_v^2(k + \gamma_v)^2 + m_v^2} c_{kv\uparrow}^\dagger c_{kv\uparrow} - \sqrt{\alpha_v^2(k - \gamma_v)^2 + m_v^2} c_{kv\downarrow}^\dagger c_{kv\downarrow}] \quad (1)$$

where the parameters α_c (α_v), m_c (m_v), and γ_c (γ_v) are used to fit the conduction (valence) bands. From this Hamiltonian, we can prove $[\hat{H}, c_{kis}^\dagger c_{kis}] = 0$ for $i = c$ or v and $s = \uparrow$ or \downarrow .

The model Hamiltonian (1) keeps the spin symmetry of the energy bands,

$$E_{i\uparrow}(k) = E_{i\downarrow}(k + Q_i) \quad (2)$$

where $Q_c = 2\gamma_c$ ($Q_v = 2\gamma_v$) is the k difference between the two conduction band bottoms (valence band tops).

We can construct the following SU(2) spin operators,

$$\begin{aligned} S_{iQ_i}^- &= \sum_k c_{ki\downarrow}^\dagger c_{(k+Q_i)i\uparrow} \\ S_{iQ_i}^+ &= \sum_k c_{(k+Q_i)i\uparrow}^\dagger c_{ki\downarrow} \\ S_i^z &= \frac{1}{2} \sum_k (c_{ki\uparrow}^\dagger c_{ki\uparrow} - c_{ki\downarrow}^\dagger c_{ki\downarrow}), \end{aligned} \quad (3)$$

where $i = c$ ($i = v$) corresponds to the conduction (valence) bands. It can be proved that these operators obey the following commutation relations.

$$\begin{aligned} [S_i^z, S_{iQ_i}^\pm] &= \pm S_{iQ_i}^\pm \\ [S_{iQ_i}^+, S_{iQ_i}^-] &= 2S_i^z \\ [H, S_{iQ_i}^\pm] &= [H, S_i^z] = 0 \end{aligned} \quad (4)$$

These results hold independently for CB and VB and there are two series of the SU(2) symmetry for both CB and VB. This commutation relation show the possibility of infinite lifetime of the spin expectation values, which is the prerequisite for the persistent spin helix. Previous research shows that injection of electron spin perpendicular to line of edge induces precession of the spin with a spatial periodicity of $l_{\text{PSH}} = \frac{2\pi}{|Q|}$. The average distance between two VBM and CBM is 0.09107 \AA^{-1} and the l_{PSH} is 6.89929 nm . This short pitch size of PSH can be used in the future development of high-density scalable spintronic devices.

IV. CONCLUSION

First, the model of PtSe₂ nanoribbon is established and the structure is determined through calculations and previous research results. The results of structure optimization shows the difference of the bold properties between

atoms near the edge and near the middle of nanoribbon. It is found that there is edge state in the nanoribbon with special zigzag edge of PtSe₂ by first-principles investigation for band structure. And the behavior band edge is similar to the fermion in vacuum which obey the law of relativity and the dispersion relation of the band edge is similar to the massive relativistic dispersion relation in a relatively large range of k space. Some mathematical methods are used to obtain fitting parameters of the band edge for further quantitative studies.

The different model which has different width of the nanoribbon is built to test the limit of the edge in nanoribbon. The result indicates that the band changes differently as number of unit cells of PtSe₂ declines which is related to the odd-even number. The analysis of the symmetry of lattice structure indicate that there is inversion symmetry for odd number and is the lack of this symmetry for even number that protects the relativistic futures of the band and keep the properties of band edge unchanged when the number of the unit cells of PtSe₂ is very small.

Further analysis was conducted reveal the relationship between edge, spin and relativistic dispersion relation. 4 of the 8 VB and CB is from one side of the nanoribbon and the remaining 4 is from the other side of the nanoribbon. For one edge of the nanoribbon, there is a horizontal spin split which is related to the Rashbar effect. Further calculation indicates that the split of spin disappears but the relativistic dispersion relation still unchanged if the SOC is not included, which can reveal the origin of the spin split. The independent Rashbar effect in the both side of the nanoribbon can induces the persistent spin helix which can be used in the spintronic devices.

ACKNOWLEDGMENTS

acknowledgments

-
- [1] K. S. Novoselov, A. K. Geim, S. V. Morozov, D.-e. Jiang, Y. Zhang, S. V. Dubonos, I. V. Grigorieva, and A. A. Firsov, *Science* **306**, 666 (2004).
- [2] A. C. Neto, F. Guinea, N. M. Peres, K. S. Novoselov, and A. K. Geim, *Reviews of Modern Physics* **81**, 109 (2009).
- [3] A. K. Geim, *Science* **324**, 1530 (2009).
- [4] M. Chhowalla, H. S. Shin, G. Eda, L.-J. Li, K. P. Loh, and H. Zhang, *Nature Chemistry* **5**, 263 (2013).
- [5] M. Chhowalla, D. Jena, and H. Zhang, *Nature Reviews Materials* **1**, 1 (2016).
- [6] Y. Wang, J. Z. Ou, S. Balendhran, A. F. Chrimes, M. Mortazavi, D. D. Yao, M. R. Field, K. Latham, V. Bansal, J. R. Friend, *et al.*, *ACS Nano* **7**, 10083 (2013).
- [7] F. A. Rasmussen and K. S. Thygesen, *The Journal of Physical Chemistry C* **119**, 13169 (2015).
- [8] M. O'Brien, N. McEvoy, C. Motta, J.-Y. Zheng, N. C. Berner, J. Kotakoski, K. Elibol, T. J. Pennycook, J. C. Meyer, C. Yim, M. Abid, T. Hallam, J. F. Donegan, S. Sanvito, and G. S. Duesberg, *2D Materials* **3**, 021004 (2016).
- [9] J. Gao, Y. Cheng, T. Tian, X. Hu, K. Zeng, G. Zhang, and Y.-W. Zhang, *ACS Omega* **2**, 8640 (2017), pMID: 31457396.
- [10] J. Li, T. Joseph, M. Ghorbani-Asl, S. Kolekar, A. V. Krashennnikov, and M. Batzill, *Advanced Functional Materials* **32**, 2110428 (2022).
- [11] Y. Wang, L. Li, W. Yao, S. Song, J. Sun, J. Pan, X. Ren, C. Li, E. Okunishi, Y.-Q. Wang, *et al.*, *Nano Letters* **15**, 4013 (2015).
- [12] W. Yao, E. Wang, H. Huang, K. Deng, M. Yan, K. Zhang, K. Miyamoto, T. Okuda, L. Li, Y. Wang, *et al.*, *Nature Communications* **8**, 14216 (2017).
- [13] S. Wagner, C. Yim, N. McEvoy, S. Kataria, V. Yokaribas, A. Kuc, S. Pindl, C.-P. Fritzen, T. Heine, G. S. Duesberg,

- and M. C. Lemme, *Nano Letters* **18**, 3738 (2018).
- [14] X. Lin, J. C. Lu, Y. Shao, Y. Y. Zhang, X. Wu, J. B. Pan, L. Gao, S. Y. Zhu, K. Qian, Y. F. Zhang, D. L. Bao, L. F. Li, Y. Q. Wang, Z. L. Liu, J. T. Sun, T. Lei, C. Liu, J. O. Wang, K. Ibrahim, D. N. Leonard, W. Zhou, H. M. Guo, Y. L. Wang, S. X. Du, S. T. Pantelides, and H. J. Gao, *Nature Materials* **16**, 717+ (2017).
- [15] Y. Zhao, J. Qiao, Z. Yu, P. Yu, K. Xu, S. P. Lau, W. Zhou, Z. Liu, X. Wang, W. Ji, *et al.*, *Advanced Materials* **29**, 1604230 (2017).
- [16] Z. Wang, Q. Li, F. Besenbacher, and M. Dong, *Advanced Materials* **28**, 10224 (2016).
- [17] C. Yim, K. Lee, N. McEvoy, M. O'Brien, S. Riazimehr, N. C. Berner, C. P. Cullen, J. Kotakoski, J. C. Meyer, M. C. Lemme, *et al.*, *ACS Nano* **10**, 9550 (2016).
- [18] C. Yim, N. McEvoy, S. Riazimehr, D. S. Schneider, F. Gity, S. Monaghan, P. K. Hurley, M. C. Lemme, and G. S. Duesberg, *Nano Letters* **18**, 1794 (2018).
- [19] L.-H. Zeng, S.-H. Lin, Z.-J. Li, Z.-X. Zhang, T.-F. Zhang, C. Xie, C.-H. Mak, Y. Chai, S. P. Lau, L.-B. Luo, *et al.*, *Advanced Functional Materials* **28**, 1705970 (2018).
- [20] J. Yuan, H. Mu, L. Li, Y. Chen, W. Yu, K. Zhang, B. Sun, S. Lin, S. Li, and Q. Bao, *ACS Applied Materials & Interfaces* **10**, 21534 (2018).
- [21] L. Tao, X. Huang, J. He, Y. Lou, L. Zeng, Y. Li, H. Long, J. Li, L. Zhang, and Y. H. Tsang, *Photonics Research* **6**, 750 (2018).
- [22] P. Chen, W. W. Pai, Y.-H. Chan, W.-L. Sun, C.-Z. Xu, D.-S. Lin, M. Chou, A.-V. Fedorov, and T.-C. Chiang, *Nature Communications* **9**, 2003 (2018).
- [23] S. Tang, C. Zhang, D. Wong, Z. Pedramrazi, H.-Z. Tsai, C. Jia, B. Moritz, M. Claassen, H. Ryu, S. Kahn, *et al.*, *Nature Physics* **13**, 683 (2017).
- [24] P. E. Blöchl, *Phys. Rev. B* **50**, 17953 (1994).
- [25] G. Kresse and J. Hafner, *Phys. Rev. B* **47**, 558 (1993).
- [26] J. P. Perdew, K. Burke, and M. Ernzerhof, *Physical Review Letters* **77**, 3865 (1996).
- [27] H. J. Monkhorst and J. D. Pack, *Phys. Rev. B* **13**, 5188 (1976).